Catalysis Communications 144 (2020) 106070

Contents lists available at ScienceDirect

Catalysis Communications

journal homepage: www.elsevier.com/locate/catcom

Short communication

Biomass-derived furfural conversion over Ni/CNT catalysts at the interface of water-oil emulsion droplets

C. Herrera[a,b], J. Pinto-Neira[a,b], D. Fuentealba[a], C. Sepúlveda[b,c], A. Rosenkranz[d], M. González[e], N. Escalona[a,b,f,g,h,*]

[a] Departamento de Química física, Facultad de Química y Farmacia, Pontificia Universidad Católica de Chile, Santiago, Chile
[b] Millenium Nuclei on Catalytic Processes towards Sustainable Chemistry (CSC), Chile
[c] Facultad de Ciencias Químicas, Casilla 160C, Universidad de Concepción, Chile
[d] Facultad de Ciencias Físicas y Matemáticas, Departamento de Ingeniería Química, Biotecnología y Materiales, Universidad de Chile, Santiago, Chile
[e] Departamento de Ingeniería y Gestión de la Construcción, Pontificia Universidad Católica de Chile, Santiago, Chile.
[f] Departamento de Ingeniería Química y Bioprocesos, Escuela de Ingeniería, Pontificia Universidad Católica de Chile, Avenida Vicuña Mackenna 4860, Macul, Santiago, Chile
[g] Unidad de Desarrollo Tecnológico, Universidad de Concepción, Coronel, Chile
[h] Centro de Investigación en Nanotecnología y Materiales CIEN-UC, Pontificia Universidad Católica de Chile, Santiago, Chile.

ARTICLE INFO

Keywords:
Hydrogenation
Furfural
Cyclopentanone
Emulsion
Carbon nanotubes

ABSTRACT

Carbon nanotubes-supported Ni catalysts were investigated for the hydrogenation of furfural as a biomass-derived furanic model compound at the liquid-liquid interface of Pickering emulsions in a batch reactor at 200 °C and 2.0 MPa of H_2 pressure. The catalysts were characterized by N_2 physisorption, He-TPD/MS, NH_3-TPD/MS, TEM, CO chemisorption, H_2-TPR, contact angle and optical/fluorescent microscopy. It was found that an increase of surface oxygen groups allows for the formation of amphiphilic particles. The amphiphilic 10%Ni/CNTox particles were homogeneous dispersed at the water-oil interface of the emulsion droplets thus enhancing the catalytic activity in furfural conversion.

1. Introduction

The reducing availability of petroleum reserves and emerging environmental concerns have generated interest in developing economically efficient and environmentally friendly technologies to transform biomass-derived molecules into fuels and chemicals [1]. Pyrolytic liquid of renewable biomass called bio-oil is a biphasic complex liquid, which is only partially soluble in either water or a hydrocarbon solvent, and contains 30% of water and more than 400 organics compounds such as phenols, guaiacols, furan and their derivatives [2,3]. Biomass-derived furanic compounds are considered as a potential platform for biofuels and chemicals thus generating notable interest regarding their upgrade possibilities. Furfural hydrogenation in the liquid phase with high H_2 pressure has been studied in monophasic systems over a variety of mono- and bimetallic catalysts on various supports [3,4]. In case of refining bio-oils for which the system is a biphasic mixture of water (30%) and non-polar molecules, the most efficient way to catalyze a reaction is to disperse an amphiphilic catalyst at the liquid/liquid interface and maximize the extent of the interface by the formation of emulsion droplets [5]. Therefore, the catalytic transformation of biomass and its derived compound (such as furfural) towards add-value chemicals requires the development of proper catalysts that act as both emulsifiers and catalysts. Recently, it has been reported that solid particles with amphiphilic character can be utilized to stabilize water-oil emulsions, which are known as Pickering emulsions [6,7]. Different parameters can affect the resulting emulsion properties [8]. The main characteristic of the amphiphilic catalysts is their ability to enhance the liquid-liquid interfacial area, which facilitates the simple separation of molecules based upon solubility differences [9]. One strategy used to synthesize an amphiphilic material is surface functionalization. It has been reported that functionalization of faujasite HY zeolites with organosilanes make able to stabilize water/oil emulsions and catalyze reactions of importance in biofuel upgrading, i.e., alkylation of m-cresol and 2-propanol in the liquid phase at high temperatures [10]. Nevertheless, despite of the positive results reported in biomass-derived conversion, the use of theses nanohybrid materials as simultaneous emulsion stabilizer and catalyst has been limited to hydrogenation of vanillin (biomass-derived polyol compounds) [11,12] and C–C

* Corresponding author at: Departamento de Química física, Facultad de Química y Farmacia, Pontificia Universidad Católica de Chile, Santiago, Chile.
E-mail address: neescalona@ing.puc.cl (N. Escalona).

https://doi.org/10.1016/j.catcom.2020.106070
Received 20 March 2020; Received in revised form 27 May 2020
Available online 05 June 2020

coupling reactions (such as aldol-condensation and alkylation reaction) over supported-Pd catalysts [13,14]. There is no report available dealing with the application of supported amphiphilic-Ni catalysts in the conversion of furfural (biomass-derived furanic compounds) in emulsion systems.

Different carbon materials such as carbonaceous microspheres, functionalized graphene and graphene oxide have been reported as effective emulsifier due to their possibility to be chemically functionalized [15]. Furthermore, these materials can be decorated with metallic nanoparticles (NPs) to enable novel catalytic activity [11,15]. It is well known that carbon nanotubes (CNT) exhibit several promising features as catalytic support due to their surface reactivity and chemical tunability achievable by functionalization [16]. In this work, the chemical oxidation of CNTs to increase their hydrophilicity was investigated followed by the study of their amphiphilic and emulsifier properties. Additionally, by doping the pristine and as-functionalized CNTs with Ni nanoparticles, their catalytic behavior in the hydrogenation of furfural, as a model biomass-derived upgrading reaction, in biphasic medium was studied.

2. Experimental section

2.1. Synthesis of catalysts

The Ni-based catalysts were supported over pristine (CNT) and functionalized CNTox. The nanohybrid catalysts were prepared by incipient impregnation of an aqueous solution of $Ni(NO_3)_2$ x $6H_2O$ with a loading of Ni (10 wt%)

2.2. Characterization of catalysts

The Ni-based catalysts were characterized by N_2 physisorption, temperature-programmed decomposition, temperature-programmed desorption of ammonia, temperature-programmed reduction, transmission electronic microscopy, CO chemisorption, static contact angles and optical/fluorescent microscopy.

2.3. Preparation of emulsion using nanohybrid catalysts

To prepare the water/oil emulsion with the 10%Ni/CNTs nanohybrid catalysts, deionized water and dodecane were used as the aqueous and organic phases, respectively.

2.4. Hydrogenation of furfural

The catalytic conversion of furfural was carried out in a Batch Parr 4561 reactor at 200 °C and 2.0 MPa of H_2 pressure. In each experiment, 0.232 mol L^{-1} of furfural, 50 mg of 10%Ni/CNTs catalyst and 16 mL of water and dodecane mixture were used. More experimental details can be found in suplementary data.

3. Result and discussion

3.1. Characterization of supports and Ni-catalysts

Table S1 (suplementary data) summarizes the BET surface area (S_{BET}), the theoretical surface area (S^*_{BET}), total pore volume (V_p) and pore diameter (d_p) of the supports and calcined Ni/CNTs catalysts. The surface area of CNTox support slightly increases after acid functionalization, suggesting that the oxidative treatment may have opened the end of CNTs [17]. Additionally, the comparison of S_{BET} and S^*_{BET} (S^*_{BET}, was calculated from the initial surface area of the support multiplied by the weight percentage of the support in each catalyst) of the 10%Ni/CNT and 10%Ni/CNTox catalysts indicates that there is no partial pore blockage after Ni incorporation. The decrease of V_p and d_p is consistent with the Ni deposition over the support.

He-TPD/MS profiles are depicted in Fig. S1a-c. Fig. S1a demonstrates that nitric acid functionalization generates an increase of the concentration of surface oxygen groups (SOG). According to CO-MS profile (Fig. S1b) these groups correspond to aldehyde (230–430 °C), carboxylic anhydride (530–680 °C), phenol/ether (600–730 °C) and carbonyl/quinone (700–900 °C) groups (weak acid and basic character). Meanwhile, the pristine CNT support presents a lower concentration of SOG, which according to CO_2-MS profile (Fig. S1c) correspond to carboxylic acid (200–430 °C), carboxylic anhydride (530–680 °C) and lactone (630–830 °C) groups (medium and strong acid character) [18].

Fig. S2 shows the NH_3-TPD/MS profile of CNT supports. It can be observed that the pristine CNT support displays a greater acidity over the entire range of NH_3 desorption temperatures compared to CNTox. This result indicates that the nitric acid modified the acidity nature of pristine CNT. The functionalization decreased the presence of medium-strong acid sites (such as lactone and carboxylic acids) of pristine CNT and favored the formation of weak and/or basic sites (such as ether and carbonyl/quinone groups) of CNTox support, which is in agreement with CO_2-MS and CO-MS profiles.

H_2-TPR profiles of calcined Ni/CNTs catalysts are shown in Fig. S3. The first reduction peak observed at 270 °C can be attributed to the reduction of NiO nanoparticles located inside of the CNTs, whereas the reduction peak registered at 360 °C can be assigned to the reduction of NiO nanoparticles dispersed in the exterior wall of CNTs, which is in agreement with the results published by Ma et al. [19]. Additionally, it has been reported that the H_2 consumption peak observed at higher temperature around 487 °C is associated with the reduction of CNTs by the formation of methane pathway [17].

TEM micrographs of the Ni/CNTs catalysts and their respective histograms of the size distribution of the Ni nanoparticles over the different CNTs supports are depicted in Fig. S4. As can be seen in Fig. S4c, some bundles appear curled after the acid treatment in the CNTox support. This suggest the effective generation of surface oxygen groups (defects), which goes hand in hand with the He-TPD/MS results [20]. Moreover, the majorities of ends of CNT are opened, which enables the deposition of Ni nanoparticles inside of the CNTs, which agrees with H_2-TPR results. However, it is important to note that both 10%Ni/CNT and 10%Ni/CNTox catalysts show deposited Ni particles inside of and onto the CNTs (see Fig. S4a,c), suggesting that the pristine CNTs had already could have opened ends naturally. The histograms of Ni particle size distribution (Fig. S4b,d) show that there is an increase of Ni nanoparticles sizes over the 10%Ni/CNTox catalyst. This result suggests that SOG with weak acidity strength such as aldehyde, carboxylic anhydride, phenol/ether and carbonyl/quinone groups promotes the increase of the sizes of the Ni nanoparticles due to weak interactions of these groups with Ni metal compared to the strong acidity of SOG present at the CNT support.

In order to estimate the metal dispersion of Ni nanoparticles, CO chemisorption was performed, and their results are summarized in Table 1. When Ni nanoparticles were deposited over CNTox a significant decrease of the CO uptake was detected. In Table 1, the dispersion expressed as CO/Ni atomic ratio is given. It can be observed that in comparison to the 10%Ni/CNT catalyst, the CO/Ni atomic ratio decreased by 2.4 times for the 10%Ni/CNTox catalyst. These results suggest that after nitric acid functionalization there is a decrease of Ni nanoparticles dispersion, which is associated to the weak acid strength

Table 1
Metal dispersion of Ni-based catalysts calculated from CO chemisorption (Ni stoichiometry of 1:1).

Catalysts	CO uptake (cm^3 g^{-1})	CO/Ni	Particle size (nm)
10%Ni/CNT	5.73	0.225	4.5
10%Ni/CNTox	2.44	0.096	10.6

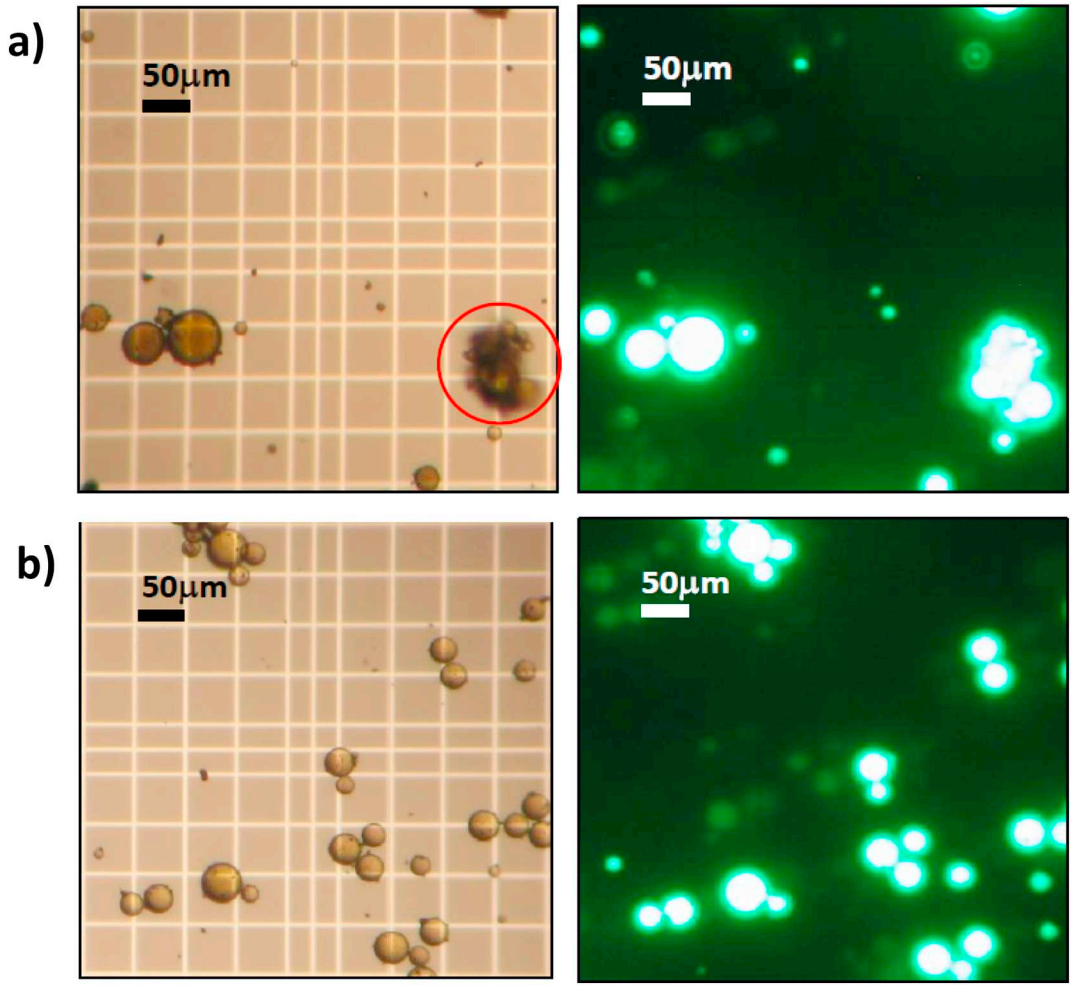

Fig. 1. Optical (left)/fluorescence (right) micrographs of emulsion droplets formed over the a) 10%Ni/CNT and b) 10%Ni/CNTox catalyst.

displayed for SOG over the CNTox support [21]. Furthermore, an increase of Ni particle size can be seen with an increasing functionalization degree of the support, in agreement with TEM results.

Static water contact angle measurements have been used to evaluate the wettability of the Ni/CNTs catalysts (Fig. S5). It has been reported that hydrophilic nanoparticles with contact angles below 90° tend to form oil-in-water emulsion (o/w), while hydrophobic nanoparticles with contact angles above 90° tend to form water-in-oil emulsion droplets (w/o) [13]. As can be seen in Fig. S5, the 10%Ni/CNT catalyst shows a contact angle of 141°, characteristic for materials with strong hydrophobic character, meanwhile the 10%Ni/CNTox catalyst shows a reduced contact angle of about 127°. These results indicate that the oxidizing treatment reduces the hydrophobic character of the CNTs making them more amphiphilic. Therefore, this result combined with He-TPD/MS points to the fact that the increase of SOG produces a reduction of the hydrophobic character to obtain an amphiphilic solid.

In Pickering emulsions, amphiphilic solid particles dispersed at the liquid-liquid interface are able to stabilize emulsion droplets [6]. To investigate the emulsifier properties of the Ni/CNTs catalysts, optical/fluorescent micrographs were obtained, and their images are shown in Fig. 1. When the mixture of water-dodecane was sonicated in presence of the 10%Ni/CNTox catalyst, the amphiphilic particles were dispersed at the liquid-liquid interface and an effective formation of emulsion droplets (droplet size, 29 μm) was observed (Fig. 1b, left). After having added a fluorescent and water-soluble dye (Fig. 1b, right), it was possible to prove that 10%Ni/CNTox catalyst forms w/o emulsion droplets, in concordance with contact angle results. In contrast, the emulsion droplets (droplet size, 37 μm) formed in presence of the 10%Ni/CNT catalyst are less stable and tend to form agglomerates of solid nanoparticles at the aqueous-organic interface (red circle, Fig. 1a), thus making the catalytic system less stable [22]. Therefore, this result highlights the key role of SOG over the surface of CNT support to improve the stability of small emulsion droplets.

3.2. Hydrogenation of furfural

Fig. S6a-b shows the conversion furfural and yield of products as a function of time over the 10%Ni/CNT and 10%Ni/CNTox catalysts, respectively. The main product obtained over both catalysts was cyclopentanone (CPO), while levulinic acid (LA) and tetrahydrofurfuryl alcohol (THF-OH) were the second major products. Trace amount of cyclopentanol (CPOL) and 2-methyltetrahydrofuran (2-MTHF) were observed. Based upon literature and the observed products, the main products produced during the hydrogenation of furfural are depicted in Fig. 2. Furfural can be converted to FUR-OH by direct C═O hydrogenation over metallic sites [23]. Then, FUR-OH can be transformed by four routes: (1) hydrogenation of C═C ring bond to form THF-OH; (2) under reduction conditions and aqueous medium, Piancantelli ring rearrangement [24] can occur to form cyclopentanone, which can be hydrogenated to cyclopentanol; (3) direct ring opening via hydrolysis to obtain LA in acid medium; and (4) dehydration to form 2-methylfuran (2-MF), which can be further hydrogenated to produce 2-MTHF. Bradley et al. [25] have shown that the relatively strong adsorption of furfural observed on metals (groups 8–10) is due to the interaction of

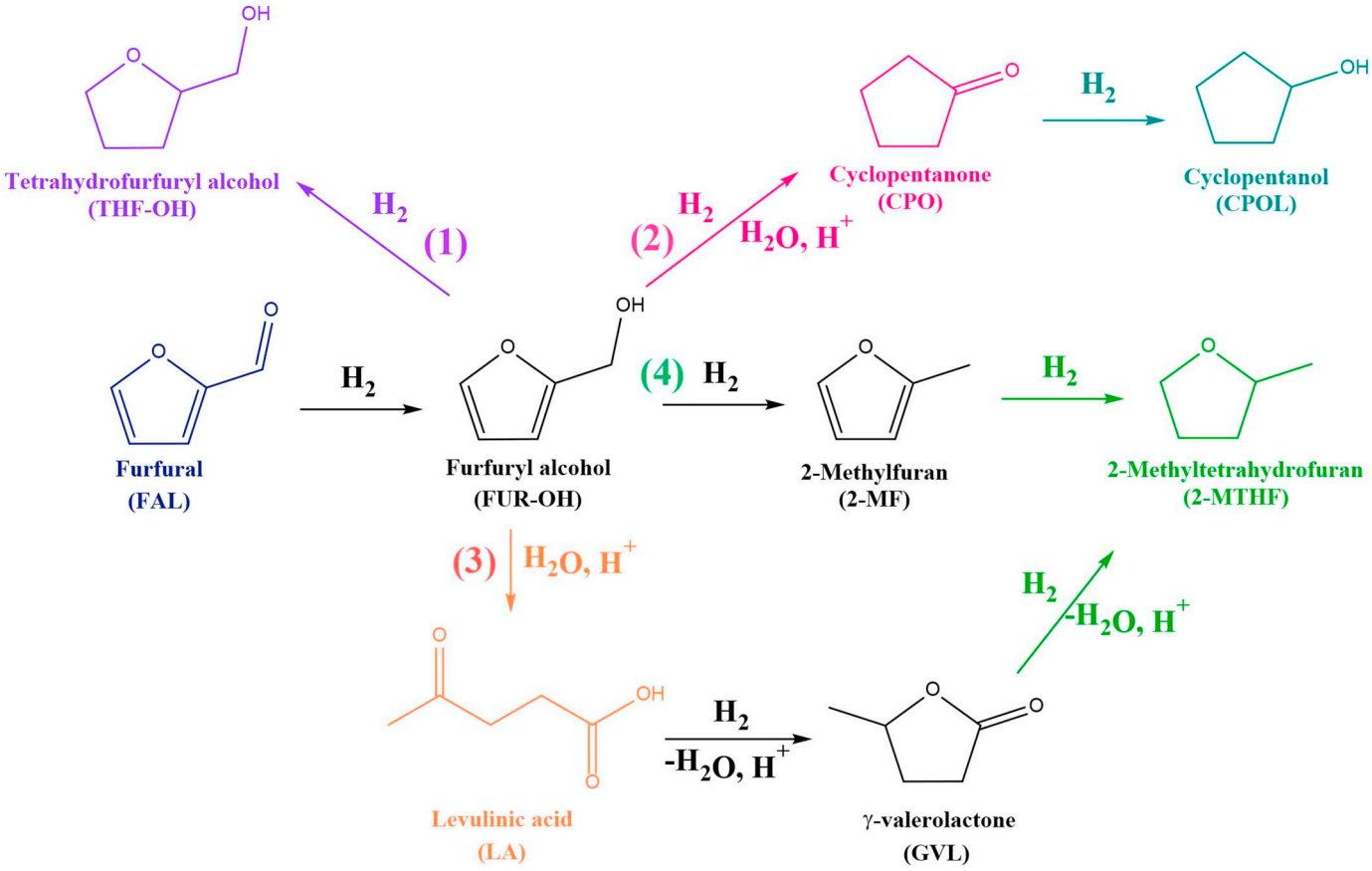

Fig. 2. Main products during the hydrogenation of furfural in water under hydrogen atmosphere and metal-acid catalysts.

the π orbitals with the metal d orbitals. This interaction weakens the C—O bond, helping to stabilize a di-sigma complex η2-(C—O) aldehyde. This behavior may explain the ring opening and rearrangement of furfural to cyclopentanone over Ni/CNTs catalysts. Furthermore, Hronec et al. have reported that when the reaction of furfural was performed under N_2 or H_2 atmosphere without catalysts, no CPO or other products were detected, which indicated that the rearrangement of the furan ring does not occur directly from furfural [26]. Moreover, it has been demonstrated that furfuryl alcohol in presence of very strong acids sites rearranged to levulinic acid (4-ketopentanoic acid) [58]. Thus, the increase of medium and strong acid sites observed by NH_3-TPD/MS over 10%Ni/CNT could favor the formation of levulinic acid at high FAL conversion, which can be further converted to 2-MTHF.

Fig. 3 shows the specific catalytic activities based upon the initial reaction rates (x 10^{-6} mol_{FAL} g_{cat}^{-1} s^{-1}) obtained from Fig. S6 and the turnover frequency (TOF) over the Ni-based catalysts. It can be observed that the initial rate over the 10%Ni/CNT catalyst is higher compared to the initial rate obtained over the 10%Ni/CNTox catalyst. This result can be attributed to an improvement of Ni nanoparticle dispersion over the CNT favored for the presence of strong SOG (such as carboxylic acids), which agrees with results of TEM, CO chemisorption and NH_3-TPD/MS. Nevertheless, TOF results show that the 10%Ni/CNTox has a catalytic activity 1.8 times greater than that obtained over the 10%Ni/CNT catalyst suggesting better activity, which is contrast to the result of the initial rate. The lower TOF obtained for the 10%Ni/CNT catalyst was attributed to the agglomerated emulsion droplets thus inducing a loss of active sites exposed, and a lower global mass transport coefficient. Jimaré et al. [27] reported that the formation of stable emulsions remarkably increases the value of the volumetric global mass transport coefficients due to the growth of the interfacial area. By

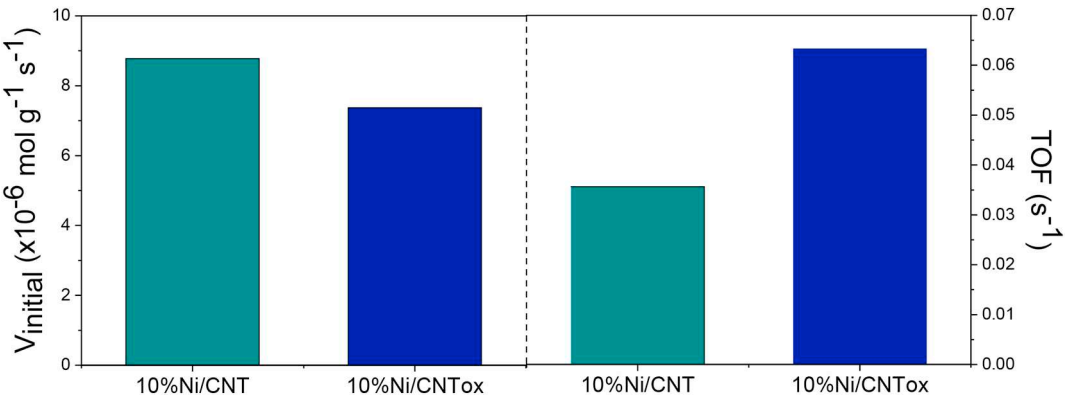

Fig. 3. Initial rate (left) and turn over frequency (TOF, right) of furfural conversion over 10%Ni/CNT and 10%Ni/CNTox catalysts, respectively.

increasing the mass transport coefficient with solid-particle stabilized emulsification the reaction rate can be greatly improved. The TOF increase indicates that significantly more FAL molecules were converted over the active sites of the 10%Ni/CNTox catalyst compared to the active sites present over the 10%Ni/CNT catalyst, although showing a lower dispersion. Therefore, this result implies that the formation of stable emulsion droplets plays a key role in enhancing the catalytic activity.

4. Conclusion

Effective catalytic hydrogenation of furfural has been investigated, in which carbon nanotube-supported nickel nanoparticles function as recoverable emulsifying agents and efficient catalysts at the same time. According to the optical/fluorescence micrographs of the reaction system, the amphiphilic 10%Ni/CNTox catalyst particles were homogeneously dispersed at the w/o interface of emulsion droplets due to the system high stability. It was found that the formation of stable emulsion droplets, achieved by the increase of SOG, plays a key role in enhancing the catalytic activity. This result offers an excellent strategy to enhance the catalytic activity in water-oil systems, which are more desirable from a practical point of view to overcome the conventional catalysis limitation for biomass and its-derived compounds (such as furfural) conversion.

Declaration of Competing Interest

The authors declare that they have no known competing financial interests or personal relationships that could have appeared to influence the work reported in this paper.

Acknowledgments

The authors are grateful to ANID-Chile for FONDECYT N° 1180982, FONDECYT N°11180121, FONDEQUIP EQM 160070, PIA CCTE AFB 170007 and CONICYT doctoral scholarship N° 21170881. The authors also gratefully thank the Chilean Ministry of Economy, Development and Tourism within the framework of the Millennium Science Initiative program for the grant “Nuclei on Catalytic Processes towards Sustainable Chemistry (CSC)”.

Appendix A. Supplementary data

Supplementary data to this article can be found online at https://doi.org/10.1016/j.catcom.2020.106070.

References

[1] M.J. Climent, A. Corma, S. Iborra, Conversion of biomass platform molecules into fuel additives and liquid hydrocarbon fuels, Green Chem. 16 (2014) 516–547, https://doi.org/10.1039/C3GC41492B.
[2] C.A. Mullen, A.A. Boateng, Chemical composition of bio-oils produced by fast pyrolysis of two energy crops, Energy Fuel 22 (2008) 2104–2109, https://doi.org/10.1021/ef700776w.
[3] Y. Nakagawa, M. Tamura, K. Tomishige, Catalytic reduction of biomass-derived Furanic compounds with hydrogen, ACS Catal. 3 (2013) 2655–2668, https://doi.org/10.1021/cs400616p.
[4] T. Tong, Q. Xia, X. Liu, Y. Wang, Direct hydrogenolysis of biomass-derived furans over Pt / CeO 2 catalyst with high activity and stability, Catal. Commun. 101 (2017) 129–133, https://doi.org/10.1016/j.catcom.2017.08.005.
[5] D. Chiaramonti, M. Bonini, E. Fratini, G. Tondi, K. Gartner, A.V. Bridgwater, H.P. Grimm, I. Soldaini, A. Webster, P. Baglioni, Development of emulsions from biomass pyrolysis liquid and diesel and their use in engines - part 1: emulsion production, Biomass Bioenergy 25 (2003) 85–99, https://doi.org/10.1016/S0961-9534(02)00183-6.
[6] M. Pera-Titus, L. Leclercq, J.M. Clacens, F. De Campo, V. Nardello-Rataj, Pickering interfacial catalysis for biphasic systems: from emulsion design to green reactions, Angew. Chem. Int. Ed. 54 (2015) 2006–2021, https://doi.org/10.1002/anie.201402069.
[7] S.U. Pickering, Emulsions, J. Chem. Soc. 91 (1907) 2001–2021, https://doi.org/10.1039/CT9079102001.
[8] Y. He, F. Wu, X. Sun, R. Li, Y. Guo, C. Li, L. Zhang, F. Xing, W. Wang, J. Gao, Factors that affect Pickering emulsions stabilized by graphene oxide, ACS Appl. Mater. Interfaces 5 (2013) 4843–4855, https://doi.org/10.1021/am400582n.
[9] M. Tang, X. Wang, F. Wu, Y. Liu, S. Zhang, X. Pang, X. Li, H. Qiu, Au nanoparticle/graphene oxide hybrids as stabilizers for Pickering emulsions and Au nanoparticle/graphene oxide@polystyrene microspheres, Carbon N. Y. 71 (2014) 238–248, https://doi.org/10.1016/j.carbon.2014.01.034.
[10] P.A. Zapata, J. Faria, M.P. Ruiz, R.E. Jentoft, D.E. Resasco, Hydrophobic zeolites for biofuel upgrading reactions at the liquid − liquid Interface in water/oil emulsions, J. Am. Chem. Soc. 134 (2012) 8570–8578, https://doi.org/10.1021/ja3015082.
[11] Z. Zhu, H. Tan, J. Wang, S. Yu, K. Zhou, Hydrodeoxygenation of vanillin as a bio-oil model over carbonaceous microspheres-supported Pd catalysts in the aqueous phase and Pickering emulsions, Green Chem. 16 (2014) 2636–2643, https://doi.org/10.1039/C3GC42647E.
[12] X. Yang, Y. Liang, Y. Cheng, W. Song, X. Wang, Z. Wang, J. Qiu, Hydrodeoxygenation of vanillin over carbon nanotube-supported Ru catalysts assembled at the interfaces of emulsion droplets, Catal. Commun. 47 (2014) 28–31, https://doi.org/10.1016/j.catcom.2013.12.027.
[13] D.E. Resasco, Carbon nanohybrids used as catalysts and emulsifiers for reactions in biphasic aqueous/organic systems, Chin. J. Catal. 35 (2014) 798–806, https://doi.org/10.1016/S1872-2067(14)60119-4.
[14] P.A. Zapata, J. Faria, M. Pilar Ruiz, D.E. Resasco, Condensation/hydrogenation of biomass-derived oxygenates in water/oil emulsions stabilized by nanohybrid catalysts, Top. Catal. 55 (2012) 38–52, https://doi.org/10.1007/s11244-012-9768-4.
[15] Y. Xie, M. Sun, Y. Shen, H. Li, G. Lv, Z. Cai, C. Yang, G.A. Ahead Ali, F. Wang, X. Zhang, Preparation of rGO-mesoporous silica nanosheets as Pickering interfacial catalysts, RSC Adv. 6 (2016) 101808–101817, https://doi.org/10.1039/C6RA22389C.
[16] E. Lam, J.H.T. Luong, Carbon materials as catalyst supports and catalysts in the transformation of biomass to fuels and chemicals, ACS Catal. 4 (2014) 3393–3410, https://doi.org/10.1021/cs5008393.
[17] A.B. Dongil, L. Pastor-Pérez, A. Sepúlveda-Escribano, R. García, N. Escalona, Hydrodeoxygenation of guaiacol: tuning the selectivity to cyclohexene by introducing Ni nanoparticles inside carbon nanotubes, Fuel. 172 (2016) 65–69, https://doi.org/10.1016/j.fuel.2016.01.002.
[18] F. De Clippel, M. Dusselier, S. Van De Vyver, L. Peng, P.A. Jacobs, B.F. Sels, Tailoring nanohybrids and nanocomposites for catalytic applications, Green Chem. 15 (2013) 1398–1430, https://doi.org/10.1039/c3gc37141g.
[19] Q. Ma, D. Wang, M. Wu, T. Zhao, Y. Yoneyama, N. Tsubaki, Effect of catalytic site position: nickel nanocatalyst selectively loaded inside or outside carbon nanotubes for methane dry reforming, Fuel. 108 (2013) 430–438, https://doi.org/10.1016/j.fuel.2012.12.028.
[20] A. Hirsch, Functionalization of single-walled carbon nanotubes, Angew. Chem. Int. Ed. 41 (2002) 1853–1859, https://doi.org/10.1002/1521-3773(20020603)41:11.
[21] C. Prado-Burguete, A. Linares-Solano, F. Rodriguez-Reinoso, C.S.M. De Lecea, Effect of carbon support and mean Pt particle size on hydrogen chemisorption by carbon-supported Pt ctalysts, J. Catal. 128 (1991) 397–404, https://doi.org/10.1016/0021-9517(91)90298-I.
[22] T. Meng, R. Bai, W. Wang, X. Yang, T. Guo, Y. Wang, Enzyme-loaded Mesoporous silica particles with tuning wettability as a Pickering catalyst for enhancing biocatalysis, Catalysts. 9 (2019) 78, https://doi.org/10.3390/catal9010078.
[23] S. Bhogeswararao, D. Srinivas, Catalytic conversion of furfural to industrial chemicals over supported Pt and Pd catalysts, J. Catal. 327 (2015) 65–77, https://doi.org/10.1016/j.jcat.2015.04.018.
[24] M. Hronec, K. Fulajtarová, T. Liptaj, Effect of catalyst and solvent on the furan ring rearrangement to cyclopentanone, Appl. Catal. A Gen. 437–438 (2012) 104–111, https://doi.org/10.1016/j.apcata.2012.06.018.
[25] M.K. Bradley, J. Robinson, D.P. Woodruff, The structure and bonding of furan on Pd (111), SUSC 604 (2010) 920–925, https://doi.org/10.1016/j.susc.2010.02.021.
[26] M. Hronec, K. Fulajtárová, T. Soták, Kinetics of high temperature conversion of furfuryl alcohol in water, J. Ind. Eng. Chem. 20 (2014) 650–655, https://doi.org/10.1016/j.jiec.2013.05.029.
[27] M.T. Jimare, F. Cazaña, A. Ramirez, C. Royo, E. Romeo, J. Faria, D.E. Resasco, A. Monzon, Modelling of experimental vanillin hydrodeoxygenation reactions in water/oil emulsions. Effects of mass transport, Catal. Today 210 (2013) 89–97, https://doi.org/10.1016/j.cattod.2012.11.015.